JACS
JOURNAL OF THE AMERICAN CHEMICAL SOCIETY
Communication
pubs.acs.org/JACS

Active and Selective Conversion of CO_2 to CO on Ultrathin Au Nanowires

Wenlei Zhu,[†] Yin-Jia Zhang,[‡] Hongyi Zhang,[†] Haifeng Lv,[†] Qing Li,[†] Ronald Michalsky,[‡] Andrew A. Peterson,*[,‡] and Shouheng Sun*[,†]

[†]Department of Chemistry and [‡]School of Engineering, Brown University, Providence, Rhode Island 02912, United States

Supporting Information

ABSTRACT: In this communication, we show that ultrathin Au nanowires (NWs) with dominant edge sites on their surface are active and selective for electrochemical reduction of CO_2 to CO. We first develop a facile seed-mediated growth method to synthesize these ultrathin (2 nm wide) Au NWs in high yield (95%) by reducing $HAuCl_4$ in the presence of 2 nm Au nanoparticles (NPs). These NWs catalyze CO_2 reduction to CO in aqueous 0.5 M $KHCO_3$ at an onset potential of −0.2 V (vs reversible hydrogen electrode). At −0.35 V, the reduction Faradaic efficiency (FE) reaches 94% (mass activity 1.84 A/g Au) and stays at this level for 6 h without any noticeable activity change. Density functional theory (DFT) calculations suggest that the excellent catalytic performance of these Au NWs is attributed both to their high mass density of reactive edge sites (≥16%) and to the weak CO binding on these sites. These ultrathin Au NWs are the most efficient nanocatalyst ever reported for electrochemical reduction of CO_2 to CO.

Selective and efficient conversion of carbon dioxide (CO_2) to a reusable form of carbon is essential for sustainable production of fuel/chemical feedstock and for balancing nature's carbon cycle to mitigate the negative impacts of overly produced CO_2. Among various methods studied for CO_2 conversion, aqueous-phase electrochemical reduction of CO_2 on metal electrocatalysts is considered clean and sustainable and has attracted much attention recently.[1] However, large negative potentials are always required for the reduction to occur,[2−5] making it impossible to perform energy-efficient conversion of CO_2 to a desired form of active carbon.[6]

Theoretical analyses of the electrochemical reduction of CO_2 have suggested that the most difficult step is not the explicit activation of CO_2 but rather the release of CO from the catalyst surface or the further conversion of CO into other active forms of carbon while suppressing competition from proton reduction to H_2.[7−12] Experimentally, it is found that nanostructured catalysts, when carefully designed and prepared, can serve as promising electrocatalysts for CO_2 reduction with improved reduction kinetics. These have been demonstrated in nanostructured Au[4] and Ag[13] for CO_2 reduction to CO, and Cu for CO reduction to ethanol.[14] Recently, a study on monodisperse polycrystalline Au NPs further suggests that the edge sites of these NPs are much more selective for CO_2 reduction to CO, while the corner sites prefer to reduce protons (from water) to H_2.[15] We hypothesize that a catalyst with one-dimensional (1D) geometry would result in an abundance of edge sites on which CO_2 can be reduced to CO. Our simple calculation indicates that when the total number of Au atoms is the same, an ultrathin 2 nm Au NW has many more edge sites but far fewer corner sites than a polyhedral NP (Figures 1a,b and S1, Supporting Information (SI)). Therefore, this Au NW should be more active for reductive CO_2 conversion to CO.

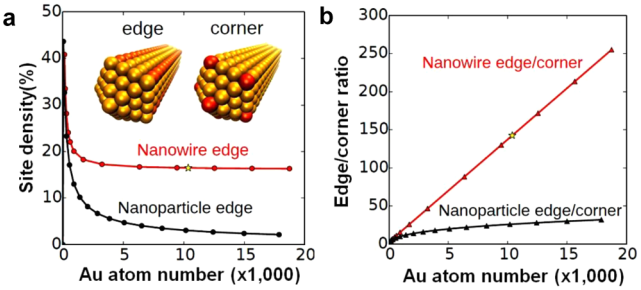

Figure 1. Catalyst model for CO_2 reduction. (a) Edge site weight percentage for a 2 nm wide Au NW and an Au NP as a function of the number of Au atoms; (b) idealized ratios of edge/corner for the Au NW and Au NP. In both figures, yellow star represents a 100 nm long Au NW corresponding to 10 377 Au atoms.

Ultrathin Au NWs can be synthesized by the reduction of Au salts in a reverse micelle-like environment.[16−20] However, small Au NPs often coexist with these NWs, making it difficult to obtain conclusive information on NW catalysis. We developed a facile seed-mediated growth method to prepare 2 nm wide Au NWs. In this approach, we first synthesized 2 nm NPs, as shown in the transmission electron microscopy (TEM) image (SI Figure S2), by reduction of $HAuCl_4$ at 60 °C in tetralin and oleylamine.[21] Au NWs were grown by reducing $HAuCl_4$ with triisopropylsilane in the presence of 2 nm Au NPs and oleylamine (SI). Figure 2a shows the TEM image of the representative ∼500 nm long and 2.1 ± 0.4 nm wide Au NWs. Compared with the NP seeds, the Au NWs show a sharper X-ray diffraction pattern (XRD) (SI Figure S3), indicating the formation of the larger face-centered cubic (fcc) domains within the NW. With the 2 nm Au NPs as seeds, the yield of Au NWs reached 95% (vs only 60% without seeds). To assess aspect-ratio effects, 100 nm long Au NWs were synthesized by

Received: September 22, 2014
Published: November 7, 2014

   dx.doi.org/10.1021/ja5095099 | J. Am. Chem. Soc. 2014, 136, 16132−16135

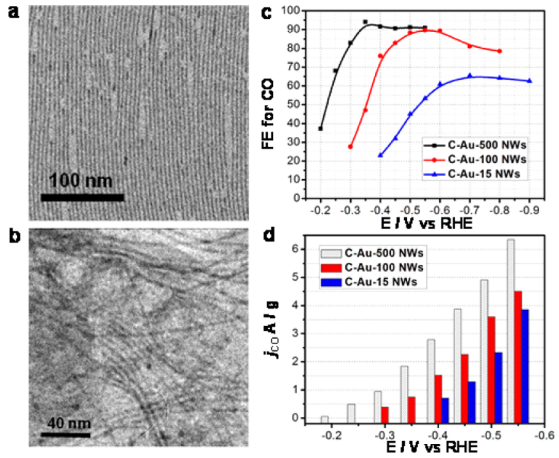

Figure 2. Au NW electrocatalysis for CO_2 reduction. (a,b) TEM images of the as-synthesized 500 × 2 nm Au NWs (a) and C−Au-500 NWs (b). The samples were prepared by depositing their hexane dispersion (a) and water suspension (b) on the carbon coated copper grids and dried in ambient conditions. (c,d) Reduction potential-dependent FE (c) and mass activity (j) (d) of the C−Au-500 NWs, C−Au-100 NWs, and C−Au-15 NWs measured in 0.5 M $KHCO_3$ from their electrochemical reduction of CO_2 to CO.

adding oleic acid into the reaction system (SI Figure S4). Long NWs could also be cut by electron (SI Figure S5) or infrared beam. For example, 30 min exposure of the 500 nm Au NWs to a 150 W infrared beam led to the formation of ∼15 nm NWs (SI Figures S3 and S6).

To study their catalytic properties, we deposited the Au NWs onto a Ketjen carbon support (mass ratio = 1) (see the SI). We designate these carbon-supported catalysts containing 500 nm long NWs, 100 nm long NWs, and 15 nm long NWs as C−Au-500, C−Au-100, and C−Au-15, respectively. The supported catalyst was immersed in acetic acid at room temperature for 24 h to remove oleylamine surfactant as described.[22] The treatment did not cause any obvious damage to the NW morphology, as indicated by the TEM images of the C−Au-500 (Figure 2b), C−Au-100 NWs (SI Figure S7a), and C−Au-15 (SI Figure S7b). The final Au/C mass ratio of the catalyst was determined by inductively coupled plasma−atomic emission spectroscopy (ICP-AES). The catalyst was ground together with polyvinylidene fluoride (PVDF) and 1-methyl-2-pyrrolidone (MP) and pasted onto a carbon paper (Toray Carbon Paper TGP-H-060) (see the SI).

The electrocatalytic reduction of CO_2 on the C−Au-500 was studied by linear sweep voltammetry (LSV) in 0.5 M $KHCO_3$ solution (pH 7.2) (SI Figure S8) to obtain the potentials required to reduce CO_2. In the following electrolysis test at a constant potential, only H_2 and CO were detected (see the SI). Figure 2c,d shows the FEs and mass activities for the formation of CO on the catalysts reported at different reduction potentials. The C−Au-500 catalyst has the CO_2 reduction onset potential of −0.2 V (with 37% FE) and the maximum FE of 94% and mass activity of 1.84 A/g Au at −0.35 V. As a comparison, the C−Au-100 and C−Au-15 have more negative onset potentials and lower FEs/mass activities. These 500 nm NWs are also much more active than the polycrystalline Au NPs reported[15] for the electrochemical reduction of CO_2 to CO.

To better understand the high activity and selectivity of the Au NWs, we studied the thermodynamic pathway of CO_2 reduction to CO, which is typically considered to consist of three elementary steps.[7,9,11,15]

$$CO_2(g) + H^+(aq) + e^- + * \rightarrow COOH* \quad (1)$$

$$COOH* + H^+(aq) + e^- \rightarrow CO* + H_2O(l) \quad (2)$$

$$CO* \rightarrow CO(g) + * \quad (3)$$

where * refers to a catalytic site at which a species can adsorb. It begins with the reductive adsorption of CO_2 on the catalyst surface leading to the formation of a COOH intermediate. The adsorbed COOH is reduced and reacts with another proton and electron, giving CO and H_2O. The first two steps are fundamentally electrochemical, each involving the transfer of an electron and a proton, and the final step is the non-electrochemical release of CO from the electrode. In previous studies,[11,15] only the first step, the conversion of CO_2 to COOH, inhibited by weak COOH binding, or the last step, the release of CO from the surface, inhibited by strong CO binding, was calculated to limit the reaction. The conversion of adsorbed COOH to adsorbed CO is typically facile.[11]

It is well-known that binding energies within a single transition metal, such as Au, Cu, or Ag, are primarily functions of the average coordination number (CN) of the binding site.[23,24] When the CN is smaller, the binding tends to be stronger. In our previous study,[15] we examined the edge site (CN = 7) on a (211) surface and the corner site (CN = 5) on a Au_{13} cluster, which suggested the edge sites had the least-rugged energy landscape for CO_2 reduction. Herein we add an explicit model of the NW geometry to enhance our understanding on structure and catalysis.[21,25−28] The 2 nm wide Au NW has a pentagonal twinned rod structure and a rich amount of edge sites (CN = 6). To classify the relative performance of these three types of CN sites, we calculated the binding energy of the adsorbed intermediates COOH and CO on the Au NW, Au(211), and Au_{13} cluster using DFT with the GPAW calculator[29] (see the SI) and present the lowest energy configurations in Figure 3a,b. Our calculations (Figure 3c,d) suggest that both COOH and CO preferentially bind to the bridge site on the Au NW edge with COOH binding marginally (0.04 eV) stronger than that on the Au(211) edge but CO binding 0.23 eV weaker than that on the Au_{13} corner. This suggests that NW surface with maximal edge sites maintains activation of CO_2 to COOH and facilitates the release of CO.

The activity of catalysts for aqueous electrochemical reduction of CO_2 often degrades with time.[4,6,14,30] We tested the stability of the C−Au-500 at a constant −0.35 V potential in the CO_2-saturated 0.5 M $KHCO_3$ (94% FE). From Figure 4a, we can see that the FE values are very stable in the first 6 h of the test, dropping only slightly after that. The morphology of the C−Au-500 after 12 h stability test was analyzed by TEM (Figure 4b), which shows a small degree of NW conversion to NPs, leading to an increase in corner sites and decrease in activity for CO formation. Despite this, these Au NWs still represent the most stable catalyst for electrochemical reduction of CO_2.

We have demonstrated a facile synthesis of ultrathin (2 nm diameter) Au NWs and studied their electrocatalysis for selective CO_2 reduction to CO in 0.5 M $KHCO_3$ solution. Au catalysts' active surfaces can be better controlled by introducing a high edge-to-corner ratio in ultrathin Au NWs to provide a lower overpotential in the pathway of CO generation and to improve the CO_2 reduction performance.

dx.doi.org/10.1021/ja5095099 | J. Am. Chem. Soc. 2014, 136, 16132−16135

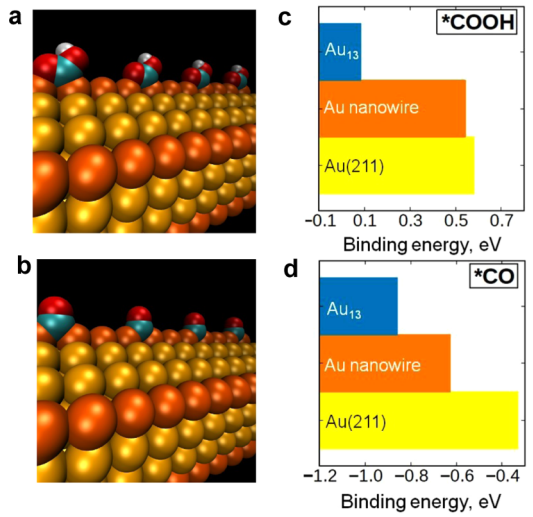

Figure 3. Computational results on CO_2 reduction and CO formation. (a,b) Configurations of the adsorbed COOH (a) and CO (b) on a Au NW. The edge-type sites are highlighted in orange. In the Au−COOH bonding mode, both C and O (carbonyl) bind to Au directly with OH tilting away from the O═C bond. In the Au−CO bonding mode, one CO binds to two Au atoms with CO serving as the bridge. (c,d) Binding energies of the key COOH (c) and CO (d) intermediates calculated on the Au NW, Au_{13} cluster, and Au(211).

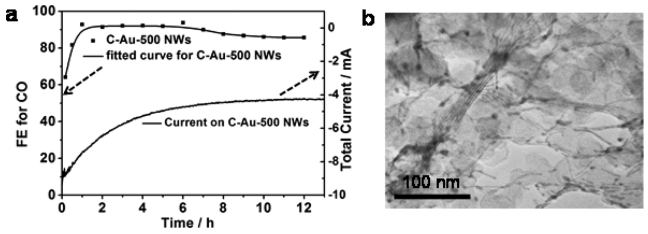

Figure 4. Au NW stability in catalyzing CO_2 reduction. (a) Time-dependent FE and the corresponding total current obtained from the C−Au-500 Au NWs at −0.35 V. (b) TEM image of the C−Au-500 NWs after 12 h stability test.

These ultrathin NWs represent a new class of catalyst for selective electrochemical reduction of CO_2 to CO (see SI Table S1 for the performance of various kinds of catalysts). The reported modeling and experimental demonstration provides a unique example in the rational design and synthesis of highly efficient catalysts for CO_2 activation and conversion.

■ ASSOCIATED CONTENT

Ⓢ Supporting Information

Materials and experimental methods, computational methods, and supplementary figures and tables. This material is available free of charge via the Internet at http://pubs.acs.org.

■ AUTHOR INFORMATION

Corresponding Authors

*andrew_peterson@brown.edu.
*ssun@brown.edu.

Notes

The authors declare no competing financial interest.

■ ACKNOWLEDGMENTS

This work was supported by the Center for the Capture and Conversion of CO_2, a Center for Chemical Innovation funded by the National Science Foundation, CHE-1240020.

■ REFERENCES

(1) Mikkelsen, M.; Jorgensen, M.; Krebs, F. C. *Energy Environ. Sci.* **2010**, *3*, 43.
(2) Zhang, S.; Kang, P.; Meyer, T. J. *J. Am. Chem. Soc.* **2014**, *136*, 1734.
(3) Kuhl, K. P.; Cave, E. R.; Abram, D. N.; Jaramillo, T. F. *Energy Environ. Sci.* **2012**, *5*, 7050.
(4) Chen, Y. H.; Li, C. W.; Kanan, M. W. *J. Am. Chem. Soc.* **2012**, *134*, 19969.
(5) Kauffman, D. R.; Alfonso, D.; Matranga, C.; Qian, H. F.; Jin, R. C. *J. Am. Chem. Soc.* **2012**, *134*, 10237.
(6) Hori, Y. *Mod. Aspects Electrochem.* **2008**, *42*, 89.
(7) Peterson, A. A.; Abild-Pedersen, F.; Studt, F.; Rossmeisl, J.; Norskov, J. K. *Energy Environ. Sci.* **2010**, *3*, 1311.
(8) Peterson, A. A.; Norskov, J. K. *J. Phys. Chem. Lett.* **2012**, *3*, 251.
(9) Nie, X.; Esopi, M. R.; Janik, M. J.; Asthagiri, A. *Angew. Chem., Int. Ed.* **2013**, *52*, 2459.
(10) Shi, C.; O'Grady, C. P.; Peterson, A. A.; Hansen, H. A.; Norskov, J. K. *Phys. Chem. Chem. Phys.* **2013**, *15*, 7114.
(11) Hansen, H. A.; Varley, J. B.; Peterson, A. A.; Norskov, J. K. *J. Phys. Chem. Lett.* **2013**, *4*, 388.
(12) Shi, C.; Hansen, H. A.; Lausche, A. C.; Norskov, J. K. *Phys. Chem. Chem. Phys.* **2014**, *16*, 4720.
(13) Rosen, B. A.; Salehi-Khojin, A.; Thorson, M. R.; Zhu, W.; Whipple, D. T.; Kenis, P. J. A.; Masel, R. I. *Science* **2011**, *334*, 643.
(14) Li, C. W.; Ciston, J.; Kanan, M. W. *Nature* **2014**, *508*, 504.
(15) Zhu, W.; Michalsky, R.; Metin, Ö.; Lv, H.; Guo, S.; Wright, C. J.; Sun, X.; Peterson, A. A.; Sun, S. *J. Am. Chem. Soc.* **2013**, *135*, 16833.
(16) Lu, X.; Yavuz, M. S.; Tuan, H.-Y.; Korgel, B. A.; Xia, Y. *J. Am. Chem. Soc.* **2008**, *130*, 8900.
(17) Huo, Z.; Tsung, C.-k.; Huang, W.; Zhang, X.; Yang, P. *Nano Lett.* **2008**, *8*, 2041.
(18) Wang, C.; Hu, Y.; Lieber, C. M.; Sun, S. *J. Am. Chem. Soc.* **2008**, *130*, 8902.
(19) Pazos-Pérez, N.; Baranov, D.; Irsen, S.; Hilgendorff, M.; Liz-Marzán, L. M.; Giersig, M. *Langmuir* **2008**, *24*, 9855.
(20) Feng, H.; Yang, Y.; You, Y.; Li, G.; Guo, J.; Yu, T.; Shen, Z.; Wu, T.; Xing, B. *Chem. Commun.* **2009**, 1984.
(21) Lee, Y.; Loew, A.; Sun, S. *Chem. Mater.* **2010**, *22*, 755.
(22) Mazumder, V.; Sun, S. *J. Am. Chem. Soc.* **2009**, *131*, 4588.
(23) Kleis, J.; Greeley, J.; Romero, N. A.; Morozov, V. A.; Falsig, H.; Larsen, A. H.; Lu, J.; Mortensen, J. J.; Dulak, M.; Thygesen, K. S.; Norskov, J. K.; Jacobsen, K. W. *Catal. Lett.* **2011**, *141*, 1067.
(24) Peterson, A. A.; Grabow, L. C.; Brennan, T. P.; Shong, B. G.; Ooi, C. C.; Wu, D. M.; Li, C. W.; Kushwaha, A.; Medford, A. J.; Mbuga, F.; Li, L.; Norskov, J. K. *Top. Catal.* **2012**, *55*, 1276.
(25) Peng, S.; Lee, Y. M.; Wang, C.; Yin, H. F.; Dai, S.; Sun, S. *Nano Res.* **2008**, *1*, 229.
(26) Johnson, C. J.; Dujardin, E.; Davis, S. A.; Murphy, C. J.; Mann, S. *J. Mater. Chem.* **2002**, *12*, 1765.
(27) Lisiecki, I.; Filankembo, A.; Sack-Kongehl, H.; Weiss, K.; Pileni, M. P.; Urban, J. *Phys. Rev. B* **2000**, *61*, 4968.
(28) Xia, Y. N.; Xiong, Y. J.; Lim, B.; Skrabalak, S. E. *Angew. Chem., Int. Ed.* **2009**, *48*, 60.
(29) Enkovaara, J.; Rostgaard, C.; Mortensen, J. J.; Chen, J.; Dulak, M.; Ferrighi, L.; Gavnholt, J.; Glinsvad, C.; Haikola, V.; Hansen, H. A.; Kristoffersen, H. H.; Kuisma, M.; Larsen, A. H.; Lehtovaara, L.; Ljungberg, M.; Lopez-Acevedo, O.; Moses, P. G.; Ojanen, J.; Olsen, T.; Petzold, V.; Romero, N. A.; Stausholm-Möller, J.; Strange, M.; Tritsaris, G. A.; Vanin, M.; Walter, M.; Hammer, B.; Hakkinen, H.; Madsen, G. K. H.; Nieminen, R. M.; Norskov, J.; Puska, M.; Rantala, T. T.; Schiotz, J.; Thygesen, K. S.; Jacobsen, K. W. *J. Phys.: Condens. Matter* **2010**, *22*, 253202.

(30) Li, C. W.; Kanan, M. W. *J. Am. Chem. Soc.* **2012**, *134*, 7231.

dx.doi.org/10.1021/ja5095099 | *J. Am. Chem. Soc.* 2014, 136, 16132−16135